Eur. Phys. J. B **41**, 383–393 (2004)
DOI: 10.1140/epjb/e2004-00331-6

THE EUROPEAN PHYSICAL JOURNAL B

Enthalpy relaxation of polymers: comparing the predictive power of two configurational entropy models extending the AGV approach

L. Andreozzi[a], M. Faetti, F. Zulli, and M. Giordano

Physics Department of University of Pisa and INFM UdR Pisa, via F. Buonarroti 2, 56127 Pisa, Italy

Received 25 February 2004
Published online 21 October 2004 –

Abstract. The Tool-Narayanaswamy-Moynihan (TNM) phenomenological model is widely accepted in order to describe the structural relaxation of glasses. However several quantitative discrepancies can be found in the literature that cannot be entirely ascribed to the experimental errors. In this work we compare the predictive power of two recently proposed configurational entropy approaches extending the TNM formalism. Both of them change the treatment of non linearity by adding a free parameter. We use Differential Scanning Calorimetry (DSC) experiments in order to test the models in two different polymers. One of them is a commercial PMMA sample, the other is a side chain liquid crystal azo-benzene polymer properly synthesized for optical nanorecording purposes. Different results were found for the two systems. In the PMMA sample only one of the new models was able to improve the agreement between DSC experiments and theory with respect to the TNM model, whereas in the second polymer both the approaches were able to describe the experiments better than TNM model.

PACS. 64.70.Pf Glass transitions – 61.43.Fs Glasses – 61.41.+e Polymers, elastomers, and plastics

1 Introduction

It is well known that glass-forming systems below their glass transition temperature T_g are in an out-of-equilibrium thermodynamic state [1]. Accordingly, if a glass is kept under isothermal condition at $T_a < T_g$ its physical properties spontaneously change and the system evolves towards its equilibrium state [2,3]. This very slow process is usually referred to as physical ageing or structural relaxation and characterizes all the different glass-forming materials. Many experimental techniques enable the study of this phenomenon, among them Differential Scanning Calorimetry (DSC) is one of the most widely used. It allows one to record the temperature dependence of the heat capacity of a sample during an heating scan through the glass transition temperature, after a complex thermal history that usually involves an annealing step in the glassy state. The recovery of equilibrium near T_g is detected, in the experimental thermograms, as an overshooting peak whose area is related to the change of enthalpy during the ageing [4]. Position and shape of the peak strongly depend on the annealing conditions. The Tool-Narayanaswamy-Moynihan model [5,6] (TNM), or the equivalent Kovacs-Aklonis-Hutchinson-Ramos (KAHR) one [7], is widely accepted in order to represent the structural recovery process in glasses. This approach takes into account the experimental finding that the kinetics of structural recovery depends on both temperature and structure of the glass that changes during the ageing. In this model the fictive temperature T_f [8], is used as structural parameter so that non-linearity is treated by assuming a specific dependence on both T_f and T of the instantaneous relaxation times. The expression originally proposed [5] is a generalized Arrhenius law:

$$\tau(T_f, T) = A \exp\left(\frac{x\Delta h}{RT} + \frac{(1-x)\Delta h}{RT_f}\right) \qquad (1)$$

where x $(0 < x < 1)$ is the non-linearity parameter partitioning the structural and thermodynamic contribution to τ, Δh is the activation energy, R the gas constant and A a prefactor. Then the Boltzmann superposition principle is assumed to be applicable during the cooling and heating procedures once a reduced time-scale is defined. As a final step, the non-exponential character of the recovery process is accounted by using the stretched exponential function as a relaxation function. In this way the constitutive equation of TNM model can be obtained in terms of the evolution of T_f [4]:

$$T_f(T) = T_0 + \int_{T_0}^{T} dT' \left(1 - \exp\left(-\left(\int_{T'}^{T} \frac{dT''}{Q\tau(T_f, T'')}\right)^{\beta}\right)\right) \qquad (2)$$

[a] e-mail: laura.andreozzi@df.unipi.it

T_0 is a reference temperature well above the glass transition temperature, Q is the cooling or heating rate and β is the stretching parameter. During the annealing step (if it exists) the second integral of equation (2) is replaced with a time integral having dt in place of dT/Q. The empirical expression defined in equation (1) has been criticized [9], and alternative relations have been proposed in literature. Among them, the most frequently used is the expression developed by Scherer [10] and Hodge [9]:

$$\tau(T_f, T) = A \exp\left(\frac{B}{RT(1 - T_2/T_f)}\right). \tag{3}$$

This latter is physically more reasonable than the previous one because at the equilibrium ($T_f = T$) the Vogel-Fulcher-Tamman law is recovered. Moreover, it can be obtained in the framework of a theoretical model by extending the Adam-Gibbs theory [11], with some ad-hoc assumptions. When equation (3) is adopted, the approach is usually named Adam-Gibbs-Vogel (AGV) model.

From the definition of the fictive temperature, the following relation is easily obtained [4]:

$$\frac{dT_f}{dT} = \frac{C_p(T) - C_p^{\text{glass}}(T)}{\Delta C_p(T_f)} \approx \frac{C_p(T) - C_p^{\text{glass}}(T)}{\Delta C_p(T)} \equiv C_p^N(T). \tag{4}$$

In equation (4), $C_p(T)$ is the heat capacity curve, $C_p^{\text{glass}}(T)$ is the unrelaxed glassy heat capacity line and $\Delta C_p(T) = C_p^{\text{liquid}}(T) - C_p^{\text{glass}}(T)$ is the heat capacity increment between the glassy and the liquid state. All these quantities can be measured experimentally by means of a DSC apparatus so that direct comparison between theoretical and experimental normalized curves (C_p^N) can be accomplished. The four model parameters (A, x, Δh and β, or T_2, B, A and β) can be conveniently found by fitting the experimental DSC traces with some search routine. Simultaneous fitting procedures of several thermograms can be conveniently adopted to reduce correlation and thermal history dependence of the model parameters [12]. However, alternative procedures to the curve fitting have also been proposed [4], which will be briefly explained in the following. In the literature usually the activation energy Δh is determined by the cooling rate dependence of the glass transition temperature [13] according to the expression:

$$\frac{\Delta h}{R} = -\frac{d \ln Q_c}{d(1/T_g)}. \tag{5}$$

From the Δh and T_g values, a crude estimation of the prefactor A is possible. To evaluate the non-linearity parameter x, the most used method is the peak shift method [14,15] where the temperature position of the DSC overshooting peak T_p, recorded after annealing the glass for a time t_a at a temperature $T_a < T_g$, is analysed as a function of the enthalpy loss $\Delta H(T_a, t_a)$ [4]:

$$\Delta H(T_a, t_a) = \int_{T_x}^{T_y} \left(C_p^a(\theta) - C_p^u(\theta)\right) d\theta. \tag{6}$$

In equation (6) $C_p^a(T)$ and $C_p^u(T)$ are the heat capacity measured after having annealed the sample at T_a for the time t_a, and the heat capacity of the unannealed sample respectively (reference scan), whereas T_x and T_y are reference temperatures ($T_x < T_g < T_y$). In a well-stabilized glass, a linear behaviour of T_p vs. ΔH is obtained, which provides the following dimensionless peak shift:

$$\hat{S} = \Delta C_p \left(\frac{\partial T_p}{\partial \Delta H}\right). \tag{7}$$

In the set of the annealing experiments, the cooling and heating rates are maintained constant. It has been shown [14,15] that this peak shift is a strong function of the non-linearity parameter x:

$$\hat{S} = F(x) \tag{8}$$

where $F(x)$ is a function almost independent of the distribution of relaxation times, theoretically calculated. The x parameter has been determined in many different glass-forming systems by using this procedure.

Finally the non-exponential parameter β can be estimated by analysing the cooling rate dependence of the upper peak [15], which is observed in intrinsic cycles, i.e. cooling-heating ramps without annealing. If an estimation of the AGV parameters (Eq. (3)) needs, some approximate expressions in terms of the TNM parameters are often used [16]:

$$x \approx 1 - T_2/T_f \approx 1 - T_2/T_g \tag{9}$$

$$\Delta h \approx \frac{B}{x^2}. \tag{10}$$

Independently of the validity of these methods in providing the values of the model parameters, in our opinion the curve fitting method has to be preferred because it allows the check of the capability of these models to describe the recovery process. Indeed, significative discrepancies that cannot be completely ascribed to the experimental errors have been observed in several polymers. These could be related to the fact that only one structural parameter, a fictive temperature, is used to model the non-linear effects. Alternative approaches and extensions of the TNM/AGV model have been proposed [17–21] where an additional parameter is introduced in modelling non-linearity. Gómez-Ribelles and coworkers have recently developed a configurational entropy approach (GR model), which better describes the DSC experiments in several polymers [21,22]. In this model, the configurational entropy $S_c(T, t)$ was used as a structural parameter. The evolution equation for S_c is formally very similar to the

constitutive equation of TNM or AGV model:

$$S_c(t) = S_c^{eq}(T_0) + \int_{T_0}^{T(t)} \frac{\Delta C_p^{lim}(\theta)}{\theta} d\theta - \sum_{i=1}^{n} \left(\int_{T_{i-1}}^{T_i} \frac{\Delta C_p^{lim}(\theta)}{\theta} d\theta \right) \exp\left(- \left(\int_{t_{i-1}}^{t_i} \frac{d\lambda}{\tau(\lambda)} \right)^{\beta} \right). \quad (11)$$

Likewise, the instantaneous relaxation times are obtained by extending the Adam-Gibbs theory

$$\tau(t) = \tau(S_c(t), T(t)) = A \exp\left(\frac{B}{S_c T} \right). \quad (12)$$

For the configurational entropy S_c and enthalpy H_c, it is assumed an identical relaxation mechanism to compare DSC experiments and theoretical curves via the relation

$$C_p(T) - C_p^{\mathrm{glass}}(T) = \frac{\partial H_c}{\partial T}. \quad (13)$$

The main difference with respect to the AGV approach is represented by the introduction in equation (11) of the term $\Delta C_p^{lim}(T) = C_p^{lim}(T) - C_p^{\mathrm{glass}}(T)$, where $C_p^{lim}(T)$ is the heat capacity of the equilibrated glass. This formalism does not assume that the limit values of configurational heat capacity in the glass, and then entropy and enthalpy, are obtained by extrapolation from the melt ($C_p^{lim}(T) = C_p^{\mathrm{liq}}$ for $T < T_g$), so that it offers the opportunity of testing different hypotheses. The simplest choice in the GR model adds one more free parameter with respect to the AGV one: it is the phenomenological shift δ of the $C_p^{lim}(T)$ with respect to $C_p^{\mathrm{liq}}(T)$. δ manifests itself in a narrow temperature range around the glass transition temperature as shown in Figure 1 [22]. We have recently shown that the GR approach describes DSC experiments in two different polymers better than other possible modifications of TNM or AGV models [23].

There is a different extension of the AGV model [24] aimed to overcome a particular flaw exhibited by this approach itself. In fact, the Adam-Gibbs temperature T_2 (see Eq. (3)) obtained directly from equation (9) or from the curve fitting method is often found at temperatures 150 K or even more below the glass transition temperature [4,24]. This appears to be physically unrealistic and disagrees with the Vogel-Fulcher temperatures usually measured by dielectric or viscoelastic investigations. This result could be related to the AGV handling of non-linearity through the assumed dependence of the out-of-equilibrium configurational entropy on the sole fictive temperature:

$$S_c(T_f) = \int_{T_2}^{T_f} \frac{\Delta C_p(\theta)}{\theta} d\theta. \quad (14)$$

With the Adam Gibbs assumption $\tau \propto \exp(B/(S_c T))$ with an hyperbolic form for $\Delta C_p(T)$ in equation (14), equation (3) is easily obtained. Because non-linearity is driven by the difference $S_c(T,t) - S_c(T)^{eq}$ it could be that equation (14) introduces too much non-linearity.

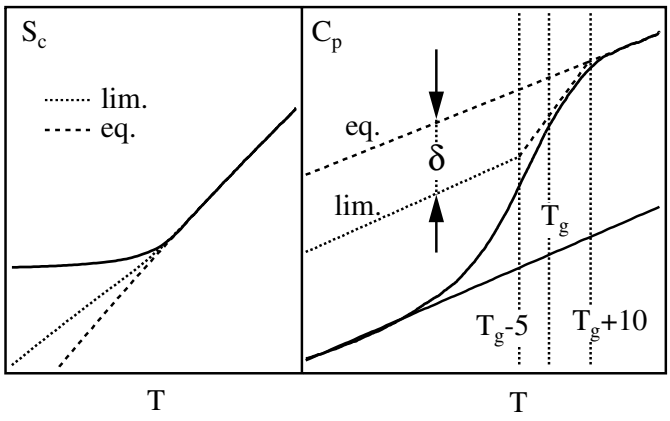

Fig. 1. The parameter δ introduced in the GR model and representing the shift in the limit glassy heat capacity with respect to its extrapolation from the melt (right). On the left, the effects on the configurational entropy are shown.

A different expression was proposed [24] where S_c depends on both fictive and present temperature through an entropic non-linearity parameter x_s, which ranges from 0 to 1:

$$S_c(T, T_f) = x_s \int_{T_2}^{T} \frac{\Delta C_p(\theta)}{\theta} d\theta + (1 - x_s) \int_{T_2}^{T_f} \frac{\Delta C_p(\theta)}{\theta} d\theta. \quad (15)$$

A possible interpretation of this expression is in terms of dynamical heterogeneities. In fact if $S_c(T_f)$, as given by equation (14), is followed during a cooling procedure, its freeze is seen at the glass transition (the glassy value of T_f). If instead the glass transition is supposed to be governed by two separate processes characterized by two different time-scales, a temperature range would exist where the behaviour of configurational entropy is intermediate between the equilibrium and the frozen one. The path followed by $S_c(T, T_f)$ would then depend on the relative weight of the two processes as in equation (15).

Equation (15) corresponds to the idea that the existence of a spectrum of relaxation times influences also the treatment of non-linearity, being related to the presence of a distribution of glass transition temperatures. The bimodal character of such distribution is solely due to a mathematical convenience and represents a simple way for taking into account the heterogeneity, via the configurational entropy. The result of equation (15) is then to provide an instantaneous relaxation time, averaged on the dynamics contribution pertaining to the faster and the slower domains. The description of the behaviour of S_c in terms of equation (15) is meaningful in a limited range of temperatures, because of the freezing of the fast component at a certain temperature T_{pf}.

It should be emphasized that the heterogeneous character of dynamics in glass-formers systems has been observed in several experimental studies [25–28]. Furthermore, in recent numerical works [29,30] the coexistence

of fast domains and slower clusters has been found in Lennard-Jones systems. More importantly, Thurau and Ediger [31], have recently evidenced the effects of spatial heterogeneities on the physical ageing mechanism of a polystyrene sample.

The approach described by equation (15) has been recently used by Saiter and coworkers [32] to study the enthalpy recovery in a semi-rigid polymer family. In a similar way Calventus and coworkers [33] found the parameters of the entropic model for some different non-stoichiometric epoxy-amine resins and discussed their physical meaning. In these works, however, no direct comparison was made between experimental DSC scans and theoretical predictions of the entropic model.

The main goal of the present work is to investigate the improvement of this new model to the AGV approach, and to compare its performance with the one of GR model in describing the physical ageing process. Both these approaches, even if in a different way, change the handling of non-linearity. According to both of them non-linearity depends on the difference $S_c(t) - S_c(t = \infty)$, but in the Hutchinson approach $S_c(t = \infty)$ coincides with the equilibrium line extrapolated from above the glass transition temperature, while in the GR model this assumption is not invoked and $S_c(t = \infty) = S_c^{lim} \neq S_c^{eq}$ is considered.

Experimental data obtained from two different polymers are here presented. For one of them, the Hutchinson model parameters are evaluated, in order to compare the two methods, by means of both the peak-shift method and the carrying out curve fitting procedures. In addition, in the light of the previous discussion of the validity of equation (15) in a narrow range of temperatures, we have assumed that the fast component of S_c freezes in abruptly at a fixed temperature.

2 Experimental details

The PMMA sample was purchased from Labservice Analytica and used as received without any further purification. Its weight average molecular weight was $M_w = 21000$ g/mol and the sample was almost monodisperse ($M_w/M_n = 1.07$). The glass transition temperature, determined according to the enthalpic definition was $T_g = 392$ K.

The second polymer is a side chain liquid crystal polymethacrylate containing a (3-methyl-4'-pentyloxy) azobenzene mesogenic unit connected at the 4-position by an hexamethylene spacer to the main chain. It was synthesized following a general literature procedure [34]. X ray measurements confirmed its nematic character in the temperature range between the glass transition $T_g = 292$ K and the clearing temperature $T_i = 353$ K. Its molecular weight distribution is characterized by $M_w \approx 59000$ g/mol and $M_n \approx 19000$ g/mol. The acronym PMA4 will be used in the following to refer to this polymer.

Differential scanning calorimetry measurements were carried out with a Perkin-Elmer DSC 7, frequently calibrated with indium and zinc standards. Highly pure nitrogen was used as purge gas. All thermal treatments were performed without removing the sample from the DSC instrument. For each polymer a single sample of about 10 mg was used. In the experiments, the samples were: i) firstly maintained at an high temperature ($T \approx T_g + 30$ K) for some minutes in order to erase any previous thermal history; ii) quenched ($Q_c = 40$ K/min) to the temperature $T_a < T_g$ and there annealed for the ageing period t_a; iii) quenched to a temperature well below the glass transition and finally reheated at the rate of 10 K/min recording the signal.

After each measurement, a reference trace was recorded following the steps i) and iii). Intrinsic cycles (cooling at different rates and heating at a fixed rate) have also been performed.

3 Results and discussion

Let us consider firstly the polymer PMMA. Its TNM parameters were estimated following the procedures described in the introduction. In Figure 2 the cooling rate dependence of its glass transition temperature is shown. According to equation (5) from these data the value of the activation energy Δh is obtained. It is found $\Delta h/R = 118 \pm 12$ kK. Moreover, from the analysis of the annealing experiments at $T_a = 382$ K $\approx T_g - 10$ K, we evaluated the non-linearity x parameter with the peak shift method.

In Figure 3 the behaviour of T_p as a function of the structural recovery of ΔH is shown. The value of 0.29 ± 0.03 was obtained for the x parameter. Finally, an estimation of the β parameter is provided by analysis of the dependence of the upper peak in intrinsic cycles, as a function of the ratio of the cooling to heating rate. In fact this peak behaves differently [15] from the main peak observed in annealing experiments, the former exhibiting sensitivity greater to the non-exponentiality parameter than to the non-linearity one. In Figure 4 two normalized experimental heat capacity curves recorded on heating after cooling at different rates are compared, whereas in Figure 5 the height of the upper peak is reported as a function of the cooling rate (at a fixed heating rate). The theoretical predictions of TNM model for two different β values are also shown (the other parameters are reported in the figure). From these data one estimates the non-exponentiality parameter β in the range $0.34 < \beta < 0.4$. The parameters of the Hutchinson model are then obtained from the relations [24]:

$$1 - x_s \approx (1 - x)\frac{T_g}{T_2} \tag{16}$$

$$B \approx \Delta h \left(1 - \frac{T_2}{T_g}\right)^2 \tag{17}$$

which can be derived following the same procedure leading to equations (9) and (10). An independent estimation of the Kauzmann or Vogel-Fulcher temperature in this sample is not available. However the WLF scaling [35] predicts $T_g - T_2 \approx 50$ K, and viscosity measurements in an almost monodisperse PMMA sample ($M_w \approx 50000$) [36]

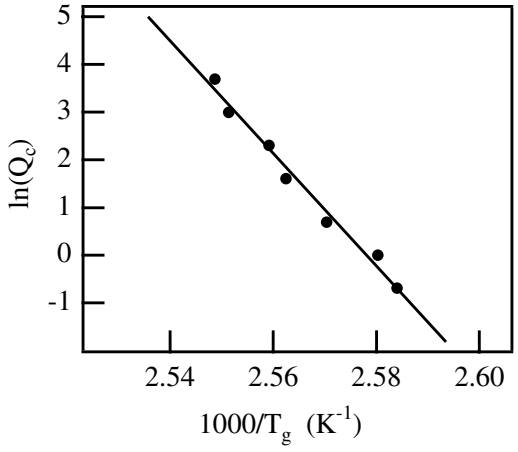

Fig. 2. Cooling rate dependence of the glass transition temperature of PMMA from simple cooling/heating experiments. According to equation (5) we found $\Delta h/R = 118 \pm 12$ kK.

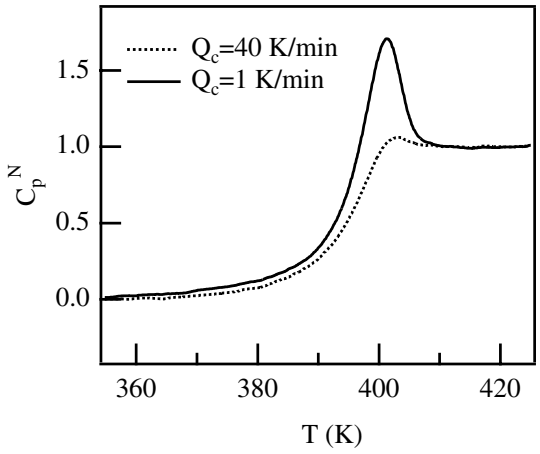

Fig. 4. Normalized DSC thermograms observed in simple cooling/heating experiments for two different cooling rates: 40 K/min (dotted line) and 1 K/min (continuous line).

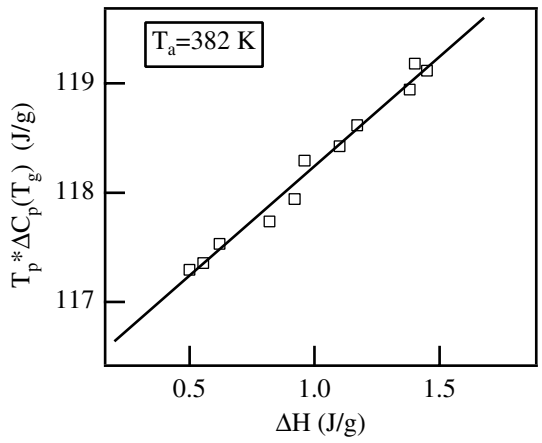

Fig. 3. Evaluation of the non linearity parameter x of TNM model through the peak shift method. Temperature of the endothermic peak, rescaled by the heat capacity change at T_g, observed in DSC traces recorded after annealing the PMMA sample at 382 K as a function of structural recovery ΔH.

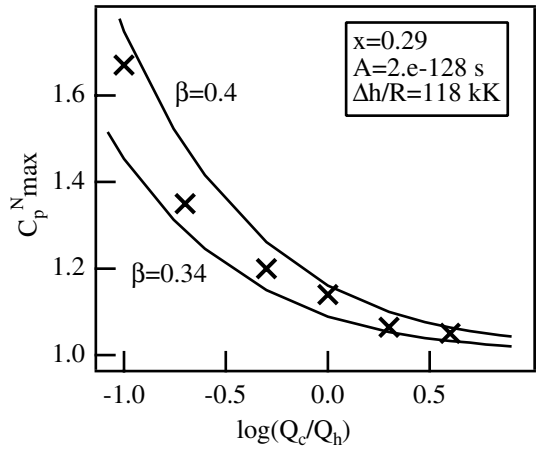

Fig. 5. PMMA sample: the maximum of the normalized DSC traces recorded during heating at 10 K/min after cooling at different rates. The lines are the predictions of TNM model as obtained for two different β values. All the parameters are reported in the figure.

provided a value of the Vogel-Fulcher temperature T_0 about 35 K below the glass transition temperature. Accordingly we attempted to fix $T_2 = 352$ K $\approx T_g - 40$ K and from equations (16) and (17), it was found $x_s \approx 0.2$ and $B/R \approx 1.2$ kK. Finally, after having assumed $\tau \approx 100$ s at the glass transition [4], the prefactor A was estimated.

We have then completed the set of parameters needed to work with the Hutchinson approach by setting $T_{pf} = T_g - 20$ K, where T_{pf} is the temperature where also the first term contributing to S_c in equation (15) is assumed to freeze in. It is important to note that the results below have appeared to be weakly dependent on the specific T_{pf} value, at least in the range $T_g - 30$ K $< T_{pf} < T_g - 10$ K.

The ability of the set of parameters to describe the recovery mechanism was tested by comparing with the corresponding theoretical curves some DSC experimental scans recorded after different thermal procedures. The comparison is shown in Figure 6 where the discrepancies appear to be very large. Because an overall temperature shift could derive from an underestimation of the prefactor A, we also arbitrarily changed it, but attempt failed in obtaining better agreement: it still remained quite poor, as shown by the dotted curves in the figure. At this stage, these results only provide an evidence that the above procedure for the evaluation of the model parameters is doubtful. In fact criticisms have been addressed on different bases. First of all, equation (5) has been criticized in a recent paper [20] where a more general expression involving also the breadth β of the relaxation time spectrum has been proposed. Furthermore, several literature studies have reported the finding that the values of Δh obtained by curve fitting are smaller than those determined by using equation (5) (Refs. in [4]).

This effect in a partial way can be traced back to the thermal lag that broadens the experimental DSC traces; however, due to the limited range of cooling rates available

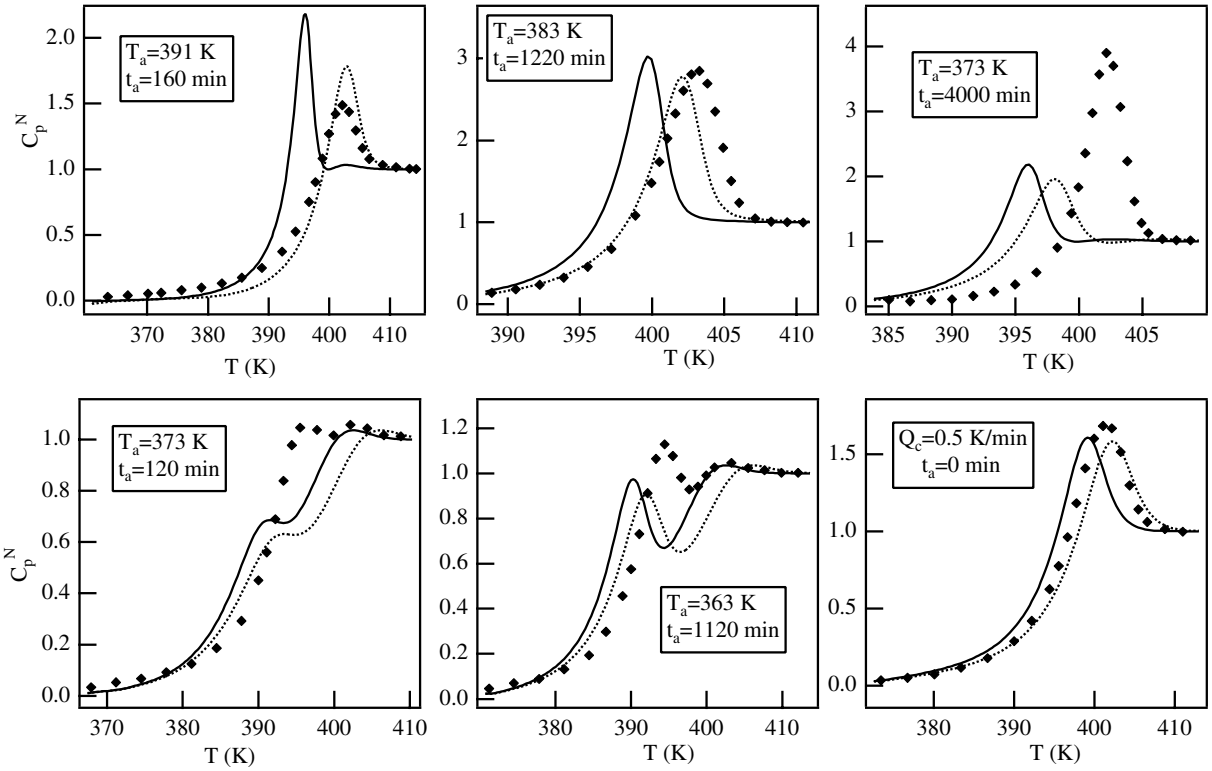

Fig. 6. Comparison between some experimental scans (diamonds) recorded after different thermal treatments of the PMMA sample and the predictions of the Hutchinson entropic model. Continuous lines are characterized by the set of parameters $A = 9.36 \times 10^{-12}$ s, $B/R = 1.2$ kK, $T_2 = 352$ K, $x_s = 0.2$ and $\beta = 0.37$. The dotted lines were obtained by using the prefactor A as a free parameter. We found $A = 5.32 \times 10^{-11}$ s.

in the experimental practice, also the error on the slope of $\ln Q_c$ vs. $1/T_g$ can be large. The second important issue is represented by the use of the peak shift method, whose applicability seems to be questionable [37]. Actually, in some cases values of x comparable with those drawn with the curve fitting method have been obtained [4]; however there is still a fundamental question, recently addressed by Zheng and coworkers [37]. By analysing a set of simulated data in the framework of TNM model, they have shown that the master curve assumed in the peak shift method is not a true master curve. The study evidenced that the error associated with the x determination from the peak shift method, strongly depends on the β value, on the different experimental variables and can be as large as 50%. They concluded that in general the curve fitting procedure has to be preferred. A final remark is devoted to the equations (9–10) or (16–17) relating the parameters of the different models, which are approximated in character because the models are not equivalent. In particular, they were derived by assuming identical behaviour of the instantaneous relaxation times as a function of temperature and fictive temperature, at the glass transition. However the shape of the overshooting peaks depends on the behaviour of the out-of-equilibrium relaxation times over the whole thermal history. This point could assume some importance, because the experimental curves in the present work involve annealing temperatures, which extend down to 30 degrees below the glass transition. These aspects could assume even more importance in the Hutchinson model, which requires an additional free parameter with respect to the TNM or AGV approach.

To get further insight we performed therefore simultaneous fitting procedures of the six experimental scans reported in Figure 6 with the different models. The Nedler-Mead search routine was employed in order to find the minimum of the function:

$$\sigma_a = \frac{1}{6N} \sum_{i=1}^{6} \sum_{j=1}^{N} \left[w(i) \left(C^N_{p,\mathrm{exp}}(i,j) - C^N_{p,\mathrm{theory}}(i,j) \right) \right]^2 . \tag{18}$$

In equation (18) the index i identifies the experimental scan whereas the index j the different points in each scan. To give the same importance to the different measurements, the weighting factors $w(i)$ were assumed proportional to the inverse of the maximum of the overshooting peaks, with $w(i) = 1$ in the case of the thermogram with highest peak. In Table 1 we report the best fit parameters of TNM model corresponding to some different values of the activation energy Δh. The last row of the table refers to the set obtained by setting $\Delta h/R = 118$ kK $x = 0.29$, values provided by the peak shift method, and $\beta = 0.37$. By inspection it is seen that the best agreement between theory and experiments is found for 78 kK $< \Delta h/R <$ 90 kK, appreciably lower than the value

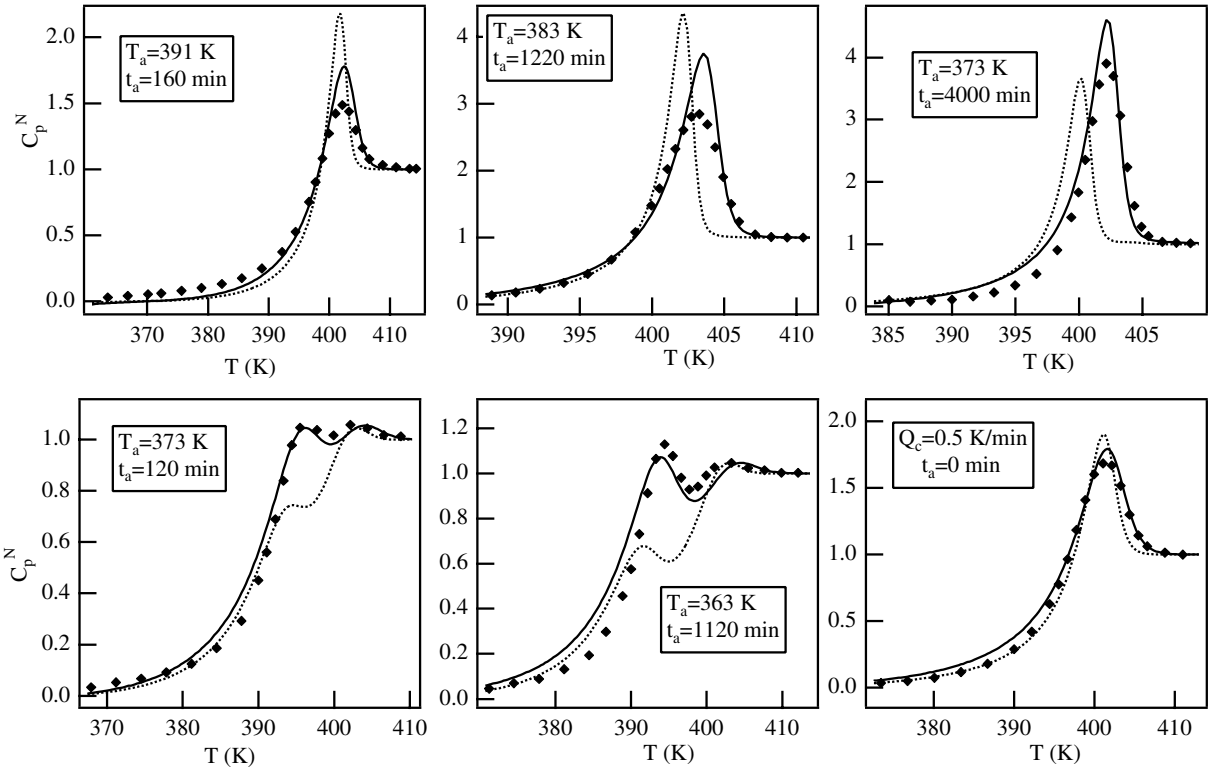

Fig. 7. Comparison between the experimental scans of Figure 6 and the best fits provided by the TNM model. The parameters are reported in Table 1 ($\Delta h/R = 84.2$ kK). The dotted lines are the predictions obtained by using the parameters reported in the last row of Table 1 and estimated through the methods described in the text.

Table 1. Best fit parameters of the TNM model for the DSC thermograms reported in Figure 6. Each set of parameters corresponds to a different value of the parameter Δh, which is fixed during the fitting procedure.

$\Delta h/R$ (kK)	A (s)	x	β	σ_a
72.2	1.6×10^{-78}	0.46	0.44	0.038
78.2	4.2×10^{-85}	0.40	0.41	0.034
84.2	1.1×10^{-91}	0.35	0.39	0.031
90.2	3.2×10^{-98}	0.31	0.36	0.035
118.0	4.0×10^{-128}	0.17	0.29	0.072
118.0	1.8×10^{-128}	0.29	0.37	0.214

$\Delta h/R = 118 \pm 12$ kK given by the analysis of the cooling rate dependence of the glass transition. Even greater discrepancies were found in other literature studies [38]. Interestingly enough, if the value $\Delta h/R = 118$ kK is set, the best fit value for the x parameter turns out to be considerably lower than the one obtained with the peak shift method. These results seem to confirm the work of Zheng and coworkers [37]. In Figure 7 the best fit traces (solid lines) according to the TNM model ($\Delta h/R = 84$ kK) are compared with the experimental ones. The predictions (dotted lines) obtained with the set of parameters originally estimated (last row of Tab. 1) are also shown.

Table 2. Best fit parameters of the AGV model in PMMA for different T_2 settings.

T_2 (K)	A (s)	B/R (K)	β	σ_a
242	1.1×10^{-32}	11810	0.42	0.030
262	6.9×10^{-30}	9416	0.39	0.029
282	2.9×10^{-26}	7070	0.36	0.034
302	4.7×10^{-23}	5152	0.34	0.043
322	8.4×10^{-19}	3344	0.31	0.054
342	5.2×10^{-14}	1860	0.29	0.061

Assuming the AGV expression provides similar agreement between theory and experiments. In Table 2 the best fit parameters found for different T_2 settings are reported. We can note that the best results correspond to an Adam-Gibbs temperature ranging in 242 K $< T_2 <$ 282 K, considerably lower than the T_g value. As next step, data were analysed in terms of the Hutchinson entropic model, to test its ability in improving the agreement with experiments and providing higher values of the Adam-Gibbs temperature. In Table 3, the best fit parameters found for some T_2 settings are reported, whereas in Figure 8 the theoretical predictions ($T_2 = 282$ K) and the experimental traces are compared. The values in the last columns of Tables 2 and 3 suggest that the entropic model does not

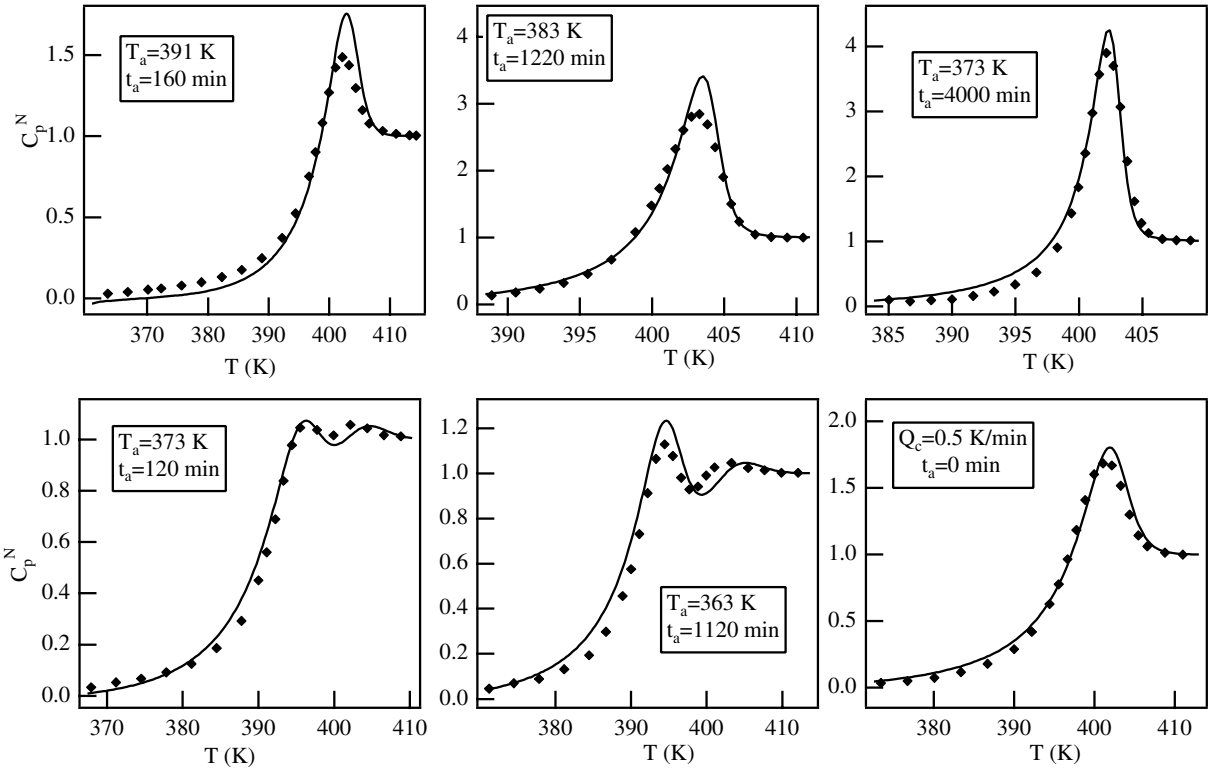

Fig. 8. Comparison between the experimental scans of Figure 6 and the best fits obtained by the Hutchinson model. The model parameters are reported in Table 3 ($T_2 = 282$ K).

significantly improve the agreement with the experimental scans with respect to the AGV approach. The possibility that this result follows from the unrealistic assumption of two separate processes governing the glass transition phenomenon was ruled out by a study carried out assuming in equation (15) x_s as a decreasing function of the temperature in the range $T_g - 20 \leq T \leq T_g$. This choice should correspond to a continuous distribution of fictive temperatures with contributions to the configurational entropy that progressively freeze on lowering the temperature.

However one could remark that, as expected, the best agreement set in the Hutchinson model presents an increased value of the Adam-Gibbs temperature, and that in the set of parameters the trend is observed that the higher the T_2 value is, the greater the corrective parameter x_s. In addition, for the highest values of the T_2 parameter, the decrement in the average square deviations is appreciable, about 25% for $T_2 = 342$ K, with respect to the set at the same T_2 in the AGV model.

To conclude our study on PMMA, the experiments are compared with the predictions of GR model, which also changes the treatment of non-linearity. Such a comparison is shown in Figure 9 ($T_2 = 282$ K), whereas in Table 4 we report the best parameters for different T_2 settings. An inspection of the results in Tables 3 and 4 evidences that GR model provides better agreement with the experiments than the Hutchinson one. It is worthwhile noting that the basic assumption of GR model has been supported in this polymer by some long term annealing experiments [23], which were found consistent with the hypothesis of a limit glassy value of enthalpy higher than its extrapolation from the melt.

To gain a further insight, we compared GR and Hutchinson approaches by using experimental data of the

Table 3. Best fit parameters of the Hutchinson model in PMMA for different T_2 settings.

T_2 (K)	A (s)	B/R (K)	β	x_s	σ_a
262	5.7×10^{-29}	9143	0.40	0.02	0.027
282	2.5×10^{-25}	6829	0.39	0.05	0.025
302	1.6×10^{-21}	4817	0.38	0.07	0.033
322	1.8×10^{-17}	3108	0.36	0.075	0.038
342	5.7×10^{-13}	1719	0.34	0.08	0.045

Table 4. Best fit parameters of the GR model in PMMA for different T_2 settings.

T_2 (K)	A (s)	B (J/g)	δ (J/gK)	β	σ_a
262	9.9×10^{-30}	4113	0.069	0.40	0.015
282	7.0×10^{-27}	2967	0.076	0.37	0.014
302	1.5×10^{-23}	2018	0.085	0.35	0.017
322	1.3×10^{-19}	1249	0.091	0.32	0.022
342	7.6×10^{-15}	657	0.094	0.30	0.030

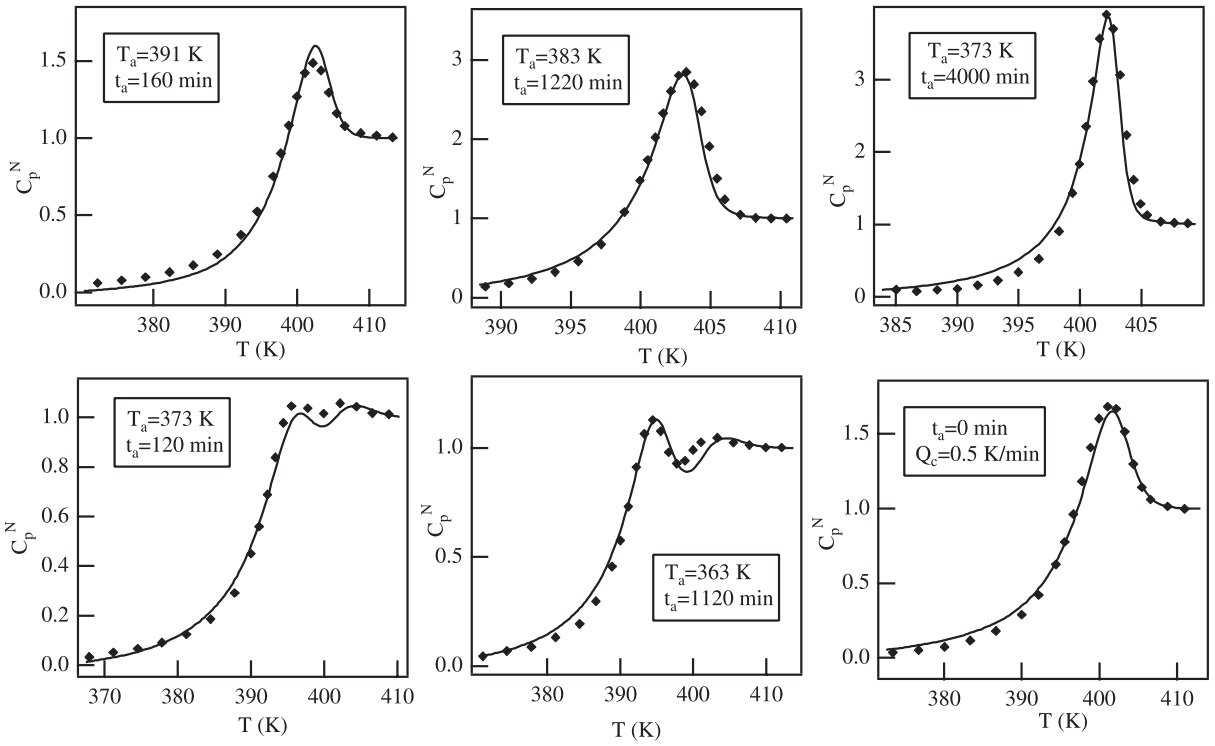

Fig. 9. Comparison between the experimental scans of Figure 6 and the best fits provided by the GR model. The model parameters are reported in Table 4 ($T_2 = 282$ K).

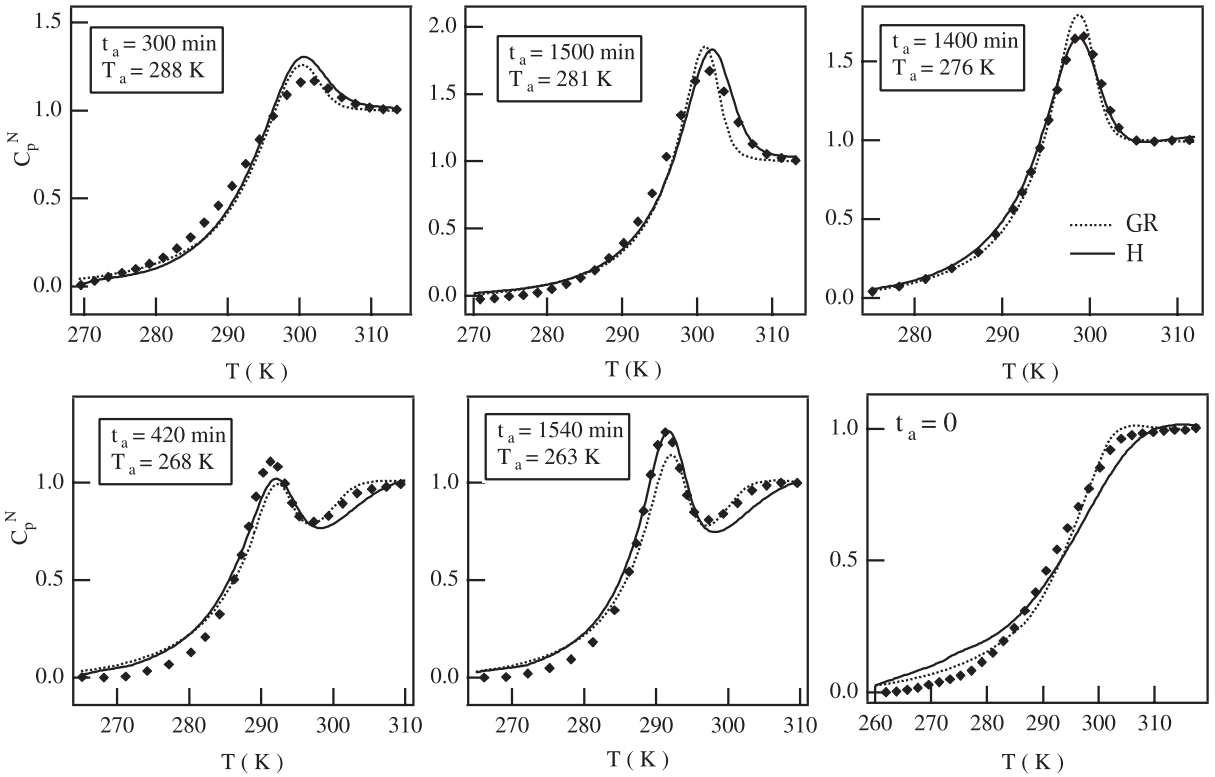

Fig. 10. Normalized heat capacity curves obtained for some different thermal treatments of the PMA4 sample compared with the best fits provided by the GR model (dotted lines) and the H approach (continuous lines). The parameters of the models are reported in Table 5.

Table 5. Best fit parameters of the AGV, GR and H models in PMA4 for different T_2 settings.

T_2 (K)	A (s)	B (J/g)	δ (J/gK)	β	x_s	σ_a	Model
227	2.2×10^{-14}	19900	-	0.26	-	0.0098	AGV
227	1.4×10^{-14}	840	0.08	0.28	-	0.0064	GR
257	2.1×10^{-6}	5294	-	0.31	0.17	0.0055	H

PMA4 polymer. The use of both the models has shown an improved description of the experiments with respect to the performances of TNM or AGV approaches. In Figure 10 the experimental thermograms are compared with the best fits obtained with the GR and H models. In this case the two approaches similarly describe the enthalpy recovery mechanism, even if, apart for the reference scan (heating at 10 K/min after a cooling at 40 K/min), H model seems to be more accurate. The previous qualitative analysis is confirmed in Table 5 where the sets of parameters providing the lowest average square deviation σ_a for the AGV, GR and H models are reported.

It is worth noting that H model provides the best value for the Adam Gibbs temperature, in good agreement with the Vogel-Fulcher temperature, $T_0 = 259 \pm 5$ K, found by viscoelastic measurements in this sample [39]. The above finding is somehow supported by the recent results from ESR studies which evidenced the highly heterogeneous character of the dynamics in this PMA4 polymer [39]. In particular, the ESR spectra of paramagnetic tracers dissolved in very low concentration in PMA4, exhibited the presence of two quite different dynamical contributions [40]. This bimodal character of the disomegeneity could be important if equation (15) is interpreted in terms of two different dynamical processes governing the glass transition.

The results of the present work seems to suggest that the H model provides an appreciable improvement in the description of the ageing mechanism only in those systems with a very high heterogeneous character of the dynamics. In particular, in PMA4 the heterogeneity is emphasized probably due to its liquid crystalline nature. More measurements on a wider set of high molecular weight polymeric materials should be carried out in order to validate this hypothesis.

Another outcome of this study is that GR model seems more general than the H approach. In fact, it was able to produce appreciable decrement of the average square deviation σ_a with respect to the AGV model in both polymers we investigated.

4 Conclusions

This work dealt with the enthalpy recovery mechanism of polymers, in particular it is devoted to the comparison of the predictive power of two recently proposed configurational entropy approaches extending the AGV model. DSC experiments performed in two different polymers were used in order to test the models. In the first part of the paper we tried to estimate the parameters of the H model for the PMMA sample, by means of the procedure widely used in literature, of the peak shift method and some approximate relations relating the TNM and the H parameters. The obtained parameters were found to be unable to reproduce the DSC thermograms. These results suggest that the curve fitting method has to be preferred to other procedures and support analogous conclusions recently published [37]. In addition, the curve fitting procedure allows one to directly compare the predictive power of the different approaches to the description of the physical aging. In the PMMA sample we showed that only the GR model highly improved the agreement between experiments and theory with respect to the AGV approach. However, if one selects the best fit parameters by looking for the minimum in the average square deviation among the experimental and the calculated DSC traces, also GR model provided an estimation of the Adam-Gibbs temperature which seems to be quite unrealistic ($T_g - T_2 = 110$ K). At variance in the side chain liquid crystal polymer experimental thermograms were described fairly well by both approaches, with only small differences between their outcomes. However the best fit values of the Adam-Gibbs temperature provided by the H model were in excellent agreement with the Vogel-Fulcher temperature obtained by viscoelastic measurements. The collection of our results does not allow a general conclusion, and suggests that a number of experimental studies on different polymers has to be carried out; however there are indications that the GR approach works better than the H model, because the former is able to describe the physical ageing experiments in both polymers investigated in the present work. In particular, the hypothesis at the basis of the GR model on the asymptotic glassy value of S_c is worthwhile of further investigation by performing very long time annealing experiments.

References

1. G.B. McKenna, S.L. Simon, in *Time Dependent and Nonlinear Effects in Polymers and composites*, edited by R.A. Schapery, C.T. Sun (American Society for Testing and Materials, West Conshohocken, PA, 2000)
2. L.C.E. Struick, *Physical aging in Amorphous Polymers and Other materials* (Elsevier, New York, 1978)
3. J.M. Hutchinson, Prog. Polym. Sci. **20**, 703 (1995)
4. I.M. Hodge, J. Non-Cryst. Solids **169**, 211 (1994)
5. C.T. Moynihan, A.J. Easteal, D.C. Tran, J.A. Wilder, E.P. Donovan, J. Am. Ceram. Soc. **59**, 137 (1976)
6. O.S. Narayanaswamy, J. Am. Ceram. Soc. **54**, 491 (1971)
7. A.J. Kovacs, J.J. Aklonis, J.M. Hutchinson, A.R. Ramos, J. Polym. Sci. **17**, 1097 (1979)

8. A.Q. Tool, J. Am. Ceram. Soc. **29**, 240 (1946)
9. I.M. Hodge, Macromolecules **20**, 2897 (1987)
10. G.W. Scherer, J. Am. Ceram. Soc. **67**, 504 (1984)
11. G. Adam, J.H. Gibbs, J. Phys. Chem. **43**, 139 (1965)
12. I.M. Hodge, A.R. Berens, Macromolecules **15**, 762 (1982)
13. C.T. Moynihan, A.J. Easteal, M.A. DeBolt, J. Tucker, J. Am. Ceram. Soc. **59**, 12 (1976)
14. J.M. Hutchinson, M. Ruddy, J. Polym. Sci. **26**, 2341 (1988)
15. J.M. Hutchinson, M. Ruddy, J. Polym. Sci. **28**, 2127 (1990)
16. I.M. Hodge, J. Res. Natl. Inst. Stand. Technol. **102**, 195 (1997)
17. A.D. Drozdov, Phys. Lett. A **258**, 158 (1999)
18. A.D. Drozdov, J. Polym. Sci. Part B: Polym. Phys. **39**, 1312 (2001)
19. I. Gutzow, D. Llieva, F. Babalievski, V. Yamakov, J. Chem. Phys. **112**, 10941 (2000)
20. J.B. Mascarell, G.G. Belmonte, J. Chem. Phys. **113**, 4965 (2000)
21. J.L. Gómez Ribelles, M. Monleón Pradas, Macromolecules **28**, 5867 (1995)
22. J.M. Meseguer Dueñas, A.V. Garayo, F.R. Colomer, J.M. Estellés, J.L. Gómez Ribelles, M. Monleón Pradas, J. Polym. Sci. B: Polymer Physics **35**, 2201 (1997)
23. L. Andreozzi, M. Faetti, M. Giordano, D. Palazzuoli, F. Zulli, Macromolecules **36**, 7379 (2003)
24. J.M. Hutchinson, S. Montserrat, Y. Calventus, P. Cortés, Macromolecules **33**, 5252 (2000)
25. H. Sillescu, J. Non-Crist. Solids **243**, 81 (1999)
26. C.Y. Wang, M.D. Ediger, J. Chem. Phys. **112**, 6933 (2000)
27. K. Schröter, E. Donth, J. Non-Cryst. Solids **307-310**, 270 (2002)
28. S.A. Reinsberg, A. Heuer, B. Doliwa, H. Zimmermann, H.W. Spiess, J. Non-Cryst. Solids **307-310**, 208 (2002)
29. C. Donati, S.C. Glotzer, P.H. Poole, W. Kob, S.J. Plimpton, Phys. Rev. E **60**, 3107 (1999)
30. S.C. Glotzer, J. Non-Cryst. Solids **274**, 342 (2000)
31. C.T. Thurau, M.D. Ediger, J. Chem. Phys. **116**, 9089 (2002)
32. A. Saiter, M. Hess, N.A.D. Souza, J.M. Saiter, Polymer **43**, 7497 (2002)
33. Y. Calventus, S. Montserrat, J.M. Hutchinson, Polymer **42**, 7081 (2001)
34. A.S. Angeloni, D. Caretti, M. Laus, E. Chiellini, G. Galli, J. Polym. Sci. Polym. Chem. Ed. **29**, 1865 (1991)
35. J.D. Ferry, *Viscoelastic properties of polymers*, 3rd edn. (John Wiley and Sons, New York, 1980)
36. R. Bergman, F. Alvarez, A. Alegria, J. Colmenero, J. Chem. Phys. **109**, 7546 (1998)
37. Y. Zheng, S.L. Simon, G.B. McKenna, J. Polym. Sci.: Part B **40**, 2027 (2002)
38. W.M. Prest Jr, F.J. Roberts, I.M. Hodge, in: *Proc. 12th NATAS Conference*, edited by J.C. Buck (NATAS, 1983), p. 119
39. L. Andreozzi, M. Faetti, M. Giordano, D. Palazzuoli, G. Galli, Macromolecules **34**, 7325 (2001)
40. L. Andreozzi, M. Faetti, M. Giordano, D. Palazzuoli, Appl. Mag. Res. **22**, 71 (2002)